Environmental Pollution 399 (2026) 128148

Contents lists available at ScienceDirect

Environmental Pollution

journal homepage: www.elsevier.com/locate/envpol

Advances in automatic airborne fungal spore monitoring: detection-efficiency test of the BAA500

Matúš Žilka [a], Samer Alashhab [b,c], Jana Ščevková [a], Carsten B. Schmidt-Weber [b,c], Inga Wessels [b,c], Jeroen Buters [b,c], Mónica González-Alonso [b,c,*]

[a] Department of Botany, Faculty of Natural Sciences, Comenius University in Bratislava, Bratislava, Slovakia
[b] Center of Allergy and Environment, Technische Universität München-Helmholtz Center, Munich, Germany
[c] Member of the German Center of Lung Research (DZL), Germany

ARTICLE INFO

Keywords:
Automatic monitoring
Efficiency
Epicoccum
Ganoderma
Alternaria
Cladosporium
Polythrincium

ABSTRACT

Fungal spores are a major component of ambient bioaerosols, contributing to environmental pollution relevant for human health, agriculture, and ecosystem management. Timely monitoring is critical, as spores can rapidly induce infections or allergic responses. Conventional Hirst-type samplers rely on time-consuming microscopic analysis, limiting near real-time reporting. Automated measurement systems offer an alternative, although their counting efficiency across fungal spore sizes and morphologies remains unclear. This study evaluates the performance of the BAA500 and Hirst-type sampler for five fungal spore types grouped by size: small (*Cladosporium*, *Ganoderma*), medium (*Epicoccum*, *Polythrincium*), and large (*Alternaria*). After genus data labelling, the BAA500 effectively discriminated all groups. The BAA500 capture efficiency was highest for medium-sized spores, capturing 2.1- and 3.4-fold higher concentrations of *Epicoccum* and *Polythrincium*, respectively, whereas small spores were underestimated more than tenfold compared to the Hirst-type sampler. The strongest correlation between devices was observed for *Alternaria* ($\rho = 0.84$), but moderate to weak for small spores. These differences likely result from sampler design, airflow rate, and optical processing algorithms. Meteorological factors influenced spore concentrations similarly for both devices, although with different magnitudes. Air temperature explained most of the variability between samplers (BAA500 is temperature-controlled, Hirst is not), and elevated spore concentrations persisted even at temperatures of 30–35 °C. These findings demonstrate the potential of automated systems for fungal spore monitoring, while highlighting the need for size-specific optimization or correction factors to improve exposure assessment across the full bioaerosol spectrum.

1. Introduction

Fungal spores dominate the microscopically visible biological fraction of atmospheric aerosols worldwide (Fröhlich et al., 2016). Despite this, they remain less studied than other airborne particles, such as pollen grains, mainly due to the lack of experts who can classify their greater taxonomic and morphological diversity and heterogeneous dispersal strategies (Després et al., 2012). Certain taxa act as potent aeroallergens and exposure to them can provoke respiratory symptoms, while others release mycotoxins and bioactive compounds with additional health implications (D'Amato et al., 2007; Straumfors et al., 2021). Beyond human exposure, many species function as phytopathogens, causing substantial crop losses and ecosystem impacts (Doehlemann et al., 2017; Martínez-Bracero et al., 2020). In addition, fungal spores may act as cloud condensation and ice nuclei, potentially affecting the Earth's radiation balance (Santarpia, 2016). Understanding the patterns of fungal spore occurrence in the air and the environmental factors driving high concentrations is therefore essential (Grinn-Gofroń and Bosiacka, 2015), particularly as climate change alters temperature regimes and atmospheric conditions that influence spore production and dispersal (Damialis et al., 2015; Williams et al., 2024). Accurate and timely detection of airborne spores is thus essential for managing biological air pollution, protecting public health, and reducing crop losses.

Traditionally, airborne fungal spores are monitored using Hirst-type volumetric samplers (Hirst, 1952) combined with light microscopic analysis. This standardized approach is robust and widely accepted

* Corresponding author. Center of Allergy and Environment, Technische Universität München-Helmholtz Center, Member of the German Center of Lung Research (DZL, Munich, Germany).
E-mail address: monica.gonzalez-alonso@tum.de (M. González-Alonso).

https://doi.org/10.1016/j.envpol.2026.128148
Received 26 February 2026; Received in revised form 1 April 2026; Accepted 14 April 2026
Available online 23 April 2026

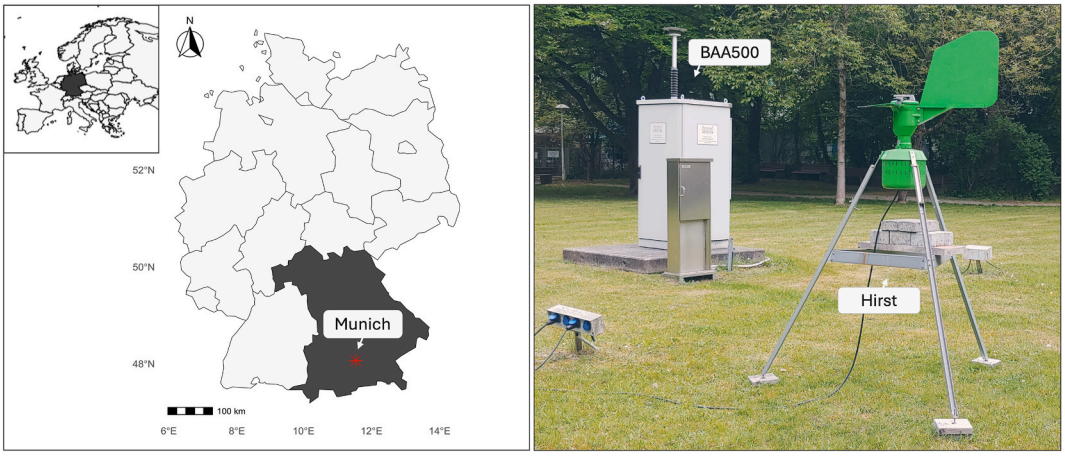

Fig. 1. Localization of sampling site with BAA500 (POMO) and Hirst-type (BURK) samplers, in the garden of Technical University of Munich.

within the aerobiology community, but it is labour-intensive and slow, with data often available only after several days or weeks (Maya-Manzano et al., 2023a). Resource limitations typically restrict reporting to daily averages, thereby reducing temporal resolution. Moreover, variability in airflow, counting methodology, and operator experience can influence the accuracy (Oteros et al., 2015; Sikoparija et al., 2017; Suarez-Suarez et al., 2023; Triviño et al., 2023). Despite these drawbacks, Hirst-type samplers remain the reference method for fungal spore quantification (Adamov et al., 2021; Galán et al., 2014; Lucas and Bunderson, 2024).

Advances in technology have led to the development of automated pollen monitoring systems that offer near-real-time analysis using principles such as digital microscopy, light scattering, fluorescence, or holography (Buters et al., 2024; Martínez-Bracero et al., 2022). Their rapid data availability, often within minutes to hours (Buters et al., 2024), is valuable for allergy prevention, early agricultural warnings, and the development of pollen forecasts. Among the earliest and most widely deployed automatic systems is the BAA500 (Hund GmbH), a virtual cascade impactor equipped with automatic image recognition capable of identifying pollen and spores. Since 2019, a network of the BAA500 samplers has been operating in Bavaria, Germany, showing high agreement with Hirst-type samplers for pollen measurements (Oteros et al., 2015, 2020; Maya-Manzano et al., 2023). For fungal spores, the classification algorithm effectively distinguishes *Alternaria* from other particles ($R^2 = 0.78$; González-Alonso et al., 2023), while all remaining fungal spores are currently grouped under a single class ("Fungus"). Visual inspection of the BAA500 image data, however, reveals substantial morphological diversity among spores, indicating that the device has the potential to detect a broader spectrum of fungal spores. Despite this potential, the capture efficiency of the BAA500 for fungal spore types other than *Alternaria* has never been systematically evaluated, and its recognition algorithm has not been trained for multi-taxon fungal spore classification. Because particle size affects sampler performance and, consequently, the measured airborne concentrations (Miki et al., 2019; Peel et al., 2014), understanding size-specific differences in detection is crucial. Airborne fungal spores range in diameter from 1 μm to 60 μm, with approximately 10 μm being the most common (Després et al., 2012).

Alternaria and *Cladosporium* are routinely monitored due to their allergenic importance and their impact on agricultural crops (Schmey et al., 2024; Zhao et al., 2024). *Cladosporium* is particularly abundant, comprising up to 90% of all airborne spores (Kasprzyk and Worek, 2006), making manual counting repetitive, time-consuming, and difficult to staff. Consequently, although more than 1000 pollen monitoring stations exist globally, only about 400 also report fungal spore counts (Buters et al., 2018). *Epicoccum* and *Polythrincium* are less frequently studied but are recognized airborne allergens (Kukreja et al., 2008; Oliveira et al., 2010) and important phytopathogens of cultivated plants (Simon et al., 2009; Jin et al., 2023). *Ganoderma* poses ecological and economic risks due to severe wood decay in forest and ornamental trees (Idris et al., 2004). Some *Epicoccum* species also exhibit biocontrol potential through antagonistic effects against plant pathogens (Taguiam et al., 2021). Monitoring these representative taxa can therefore yield valuable information relevant to public health and agriculture management.

Given the ecological, medical, and agricultural importance of these spores and the need for reliable automated sampling tools, this study aims to evaluate size-dependent performance the BAA500 for five environmentally and clinically relevant fungal spore taxa, having the Hirst-type sampler as a reference.

2. Materials and methods

2.1. Study area

The comparison campaign between the two monitors was conducted in the garden of the Technical University of Munich (TUM), adjacent to the Centre of Allergy and Environment (ZAUM) building in Munich, Germany (48.164588, 11.593196), from 26 April to 15 October 2024 (Fig. 1). The site consists of a grass field surrounded by some *Tilia* trees and buildings. The BAA500 (hereinafter POMO) sampler was placed in the centre of the garden, while a Hirst-type trap (Burkard Manufacturing Co Ltd; hereinafter BURK) was positioned 5 m away. Although the POMO location may not represent a larger area, it was considered suitable for the objectives of this study, as the device is primarily used for research purposes, here the comparison with a Hirst-type trap located within 5m. The POMO inlet is approximately 2 m above ground level, and the BURK inlet was located at about 1.5 m a.g.l.

2.2. Aerobiological sampling methods

Both samplers operate on a similar principle: air is drawn in by a pump, particles impact on an adhesive surface, and are subsequently identified – either using microscopy by an expert (BURK) or by an image-recognition algorithm (POMO).

The BURK trap operated at a mean air flow rate of 10 L/min, measured resistance-free with a hand-held anemometer (Cavazza Ana easyFlux® heat-flowmeter, Italy). Particles were collected through a 2 × 14 mm slit on an adhesive tape moving at a rate of 2 mm/h. Sampling was conducted using a 7-day drum. Once a week, the drum was replaced, and the Vaseline-coated (Melinex®) tape was cut into segments, each corresponding to a 24-h exposure period. Microscope slides

were mounted using glycerogelatin stained with safranin, which selectively stains pollen grains but not fungal spores, to enhance contrast and improve spore differentiation. Analyses were carried out in cooperation with the Department of Botany, Comenius University in Bratislava. Fungal spore identification followed the atlases of Lacey and West (2006), Li et al. (2023), and Smith (2000), and concentrations were calculated following the recommendations of the European Aerobiology Society guidelines (Galán et al., 2014) and the European standard EN 16868:2019, with a 2-h temporal resolution.

The POMO is an image recognition-based virtual cascade impactor that samples ambient air at a flow rate of 1120 L/min 90% of the inlet flow is discarded as it only serves to protect pollen from hitting the wall and sticking there, resulting in a sampled airflow of 100 L/min. As the sampler has an on/off rhythm of 1 min on and 9 min off, to prevent slide overload, the effective airflow is approximately 10 L/min (constantly monitored). The sampler is designed to exclude particles smaller than 5 μm, thereby reducing interference from non-pollen aerosols (Plaza et al., 2025; Buters et al., 2024). Airborne particles impact an adhesive plate, which is subsequently heated to allow particles to embed into and rehydrate within the gelatin substrate. A randomly selected 33% portion of the slide area is then imaged by a microscope camera every 3 h. During each cycle, the system captures approximately 144 regions of the sticky plate, with each region producing a stack of ~180 images along the z-axis. Each stack is condensed into a single synthetic grayscale image (1280 × 960 pixels).

Detected particles are automatically classified into pollen taxa, *Alternaria,* a general "Fungus" group (all remaining fungal spores combined), or non-pollen particles. All images are stored in an online NoSQL (MongoDB) database to ensure efficient data handling and retrieval.

2.3. Sample analysis and capture efficiency comparison

To evaluate capture efficiency across the size range of the studied spores, we compared the total amount of the selected spores sampled by each sampler, calculated doing the sum of all five types per sampler. For the study, we selected spores with geometric diameters of 3-11 μm (*Cladosporium, Ganoderma*), 15-25 μm (*Epicoccum, Polythrincium*), and >20 μm (*Alternaria*) (Li et al., 2023), representing four Ascomycetes and one Basidiomycete (*Ganoderma*).

Currently, the POMO software automatically identifies only *Alternaria* spores. Therefore, the remaining four taxa were manually labelled using the digital platform "validation.pollenscience.eu" (https://validation.pollenscience.eu/). The platform enables filtering particle images by date, visualizing them, and manually assigning classes to individual particles by experts – a process referred to as labelling. Labelling and counting were conducted in collaboration with the Department of Botany at Comenius University in Bratislava. To minimize bias, all BURK samples and all POMO images were analysed by the same expert throughout the sampling period.

Data normality was assessed using the Shapiro–Wilk test. Since BURK provides 2-h data and POMO provides 3-h data, both datasets were aggregated to 6-h intervals for direct comparison. Differences and agreement between the two devices were evaluated using the Wilcoxon signed-rank test and Bland-Altman analysis, respectively. Spearman correlation and redundancy analysis (RDA, including meteorological variables) were used for further comparisons. Descriptive analyses were used to investigate temporal patterns of the five spore taxa, and diurnal patterns were examined to determine whether differences existed between devices.

All datasets were synchronized to a common time zone and unified to a single timestamp format. Due to technical or logistical interruptions from either instrument, data from 32 out of 172 days were excluded (30 May–3 June, 5–6 June, 8–12 June, 14–15 June, 24 June, 30 June, 3 July, 5–6 July, 15 July, 26 July, 21–22 August, 26–29 August, 29–30 September, and 2–4 October)(Fig. S1).

Table 1
Total number of spores included in the size analysis for each spore type.

Spore type	Sample size labelled	Sample size clean	Difference	Difference (%)
Alternaria	1888	1090	798	42.3
Cladosporium	7996	7365	632	7.9
Epicoccum	4485	4430	55	1.2
Ganoderma	135	129	6	4.4
Polythrincium	5806	5653	153	2.6

Sample size labelled – total number of spores manually labelled through the web interface; *Sample size clean* – number of spores used for size analysis after removal of segmented or damaged spores; *Difference* – number of spores excluded from size analysis; *Difference (%)* – proportion of spores excluded from size analysis.

2.4. Spore size analysis

To assess the impact of spore size on POMO's capture efficiency, we analysed the size distribution of the sampled spores. The POMO software employs a Mask R-CNN–based image segmentation module to detect and count particles on synthetic grayscale images, generating bounding boxes around each particle. The bounding box coordinates (x, y, width, height) were used to extract regions of interest (ROIs), representing individual spores, and to derive morphological measurements, such as width, height, perimeter, and orientation angle.

Binary masks were applied to isolate spores from the background using pixel-wise segmentation, combined with adaptive thresholding to remove uniform background noise. When contour detection failed, alternative thresholds (160–240, or if needed, 0–10) were applied. The cleaned binary images were then processed to detect contours, from which rotated minimum-area bounding rectangles were fitted, enabling the extraction of key morphological features (Fig. S2).

Pixel dimensions were converted to micrometres using calibration factors based on camera resolution (1280 × 960 pixels) and microscope magnification (400 ×), resulting in a pixel size of 0.3125 μm (width) and 0.4167 μm (height).

Morphological data and manual labels were processed in Python using the Pandas library. Rows with missing key values were excluded to ensure data robustness. For each fungal spore type, descriptive statistics were calculated, including sample size, range, percentiles, and Tukey fences to identify outliers based on the interquartile range (Tukey and John, 1977). All values represent measurements from spores captured under environmental conditions.

Size distribution patterns were analysed by fitting log-transformed measurements to log-normal probability density functions (PDFs) using maximum likelihood estimation. The resulting curves were overlaid on histograms to visualize differences among taxa (Fig. S3). In cases where the segmentation mask captured only part of a spore, images were manually excluded. This issue was most pronounced in *Alternaria*, where ~42% of measurements were removed because the mask missed the characteristic spore tail (Table 1).

2.5. Influence of meteorological variables

The influence of meteorological factors on spore concentrations and seasonality was assessed using Redundancy analysis (RDA) and Spearman correlations. Spearman correlations were calculated separately for each trap. Since temperature was identified as the most influential weather variable, we conducted a further analysis comparing temperature ranges and spore abundances.

Since there was no weather station at the sampling site, meteorological parameters were obtained from the nearest station (Helene Weber Allee, Munich; 48.1635°N, 11.5437°E) of the German Weather Service (DWD), which is located 7 km apart. Data were obtained from the DWD Open Data Center (https://opendata.dwd.de/climate_environment/CDC/observations_germany/). Hourly data of air

Table 2
Descriptive statistics of meteorological parameters during the study period.

Statistic	AT	RH	R	AP	GT	WS	WD	SD
Minimum	0.5	17	0	931.4	5	0.4	0	0
Median	16	76.5	0	954.6	18.4	2.2	220	3
Maximum	33.3	100	18	971.6	36.7	9.6	360	60
Mean	16.2	72.6	0.2	954.6	18.7	2.5	191.3	21.7

AT – air temperature (°C); *RH* – relative humidity (%); *R* – rainfall (mm); *AP* – air pressure (hPa); *GT* – ground temperature (°C); *WS* – wind speed (m/s); *WD* – wind direction (°); *SD* – sunshine duration (hourly sum, in minutes).

temperature (°C), relative humidity (%), rainfall (mm), air pressure (hPa), ground temperature (°C), wind speed (m/s), wind direction (°), and sunshine duration (hourly sum, in minutes) were collected at a height of 2 m. Summary statistics of the meteorological parameters are presented in Table 2.

2.6. Software

Data analysis and visualization were performed using R (R Core Team, 2024) and Python (Python Software Foundation, 2024). In R, the following packages were used: *blandr*, *vegan*, *corrplot*, *ggpubr*, and *ggplot2*. Python analyses employed *NumPy*, *Pandas*, *SciPy*, *Seaborn*, and *Matplotlib*.

The fungal spore data and the code used for processing and statistical analyses are available in the Zenodo repository at 10.5281/zenodo.17985095.

3. Results

3.1. Comparison of capture efficiency

Total fungal spores recorded by POMO during the campaign ranged from 495 for *Ganoderma* (0.6%) to 27,519 for *Cladosporium* (35.1%). In the BURK sampler, total spore counts ranged from 2923 for *Polythrincium* (1.7%) to 138,636 for *Cladosporium* (79.5%) (Table 3). The mean daily concentrations were highest for *Cladosporium* in both samplers, while the lowest values were observed for *Ganoderma* in POMO and *Polythrincium* in BURK. Three of the five taxa reached their seasonal maximum on the same day, whereas *Cladosporium* and *Ganoderma* differed markedly in peak timing.

Diurnal variation was analysed in 6-h intervals to ensure comparability between devices. Most taxa showed higher concentrations between 06:00 and 18:00 in both samplers, except for *Ganoderma*, which exhibited a clear nocturnal maximum, peaking between 18:00–00:00 in POMO and 00:00–06:00 in BURK (Fig. 2). No significant differences in the timing of diurnal peaks between samplers were detected.

Comparison of total 6-hourly spore concentrations using the Wilcoxon test revealed significant differences for all taxa ($p < 0.001$), except for *Alternaria* ($p = 0.077$). Bland-Altman analysis showed strong agreement between devices for *Alternaria*, moderate agreement for *Epicoccum* and *Polythrincium*, and low agreement for *Cladosporium* and *Ganoderma*. Overall, spore concentrations were significantly higher in the BURK sampler, mainly due to elevated counts of small-sized spores such as *Cladosporium* and *Ganoderma* (Fig. 3). In contrast, POMO recorded higher abundances of medium-sized spores (*Epicoccum*, *Polythrincium*), while *Alternaria* exhibited comparable concentrations with slightly higher values in POMO.

Spearman correlation analysis between devices at 6-h resolution showed strong associations for *Alternaria* ($\rho = 0.67$), *Epicoccum* ($\rho = 0.68$), and *Polythrincium* ($\rho = 0.68$), moderate associations for *Cladosporium* ($\rho = 0.49$) and total spore counts ($\rho = 0.61$), and a weak association for *Ganoderma* ($\rho = 0.17$) (Fig. S4). Aggregation to daily resolution improved correlations by an average of 0.15 across taxa, with the largest increases observed for *Ganoderma* (+0.29) and *Alternaria* (+0.17). At daily resolution, correlations were highest for *Alternaria* ($\rho = 0.84$), *Polythrincium* ($\rho = 0.79$), *Epicoccum* ($\rho = 0.74$), and total (summed) spore counts ($\rho = 0.73$), while *Cladosporium* remained moderate ($\rho = 0.59$) (Fig. 4).

3.2. Spore size distribution

Measurements of spore width, height, and perimeter revealed the greatest variability for *Alternaria* and the lowest for *Ganoderma*. This likely reflects the smaller sample size of *Ganoderma* (129 spores) and the broad morphological variability within *Alternaria* (1090 spores) (Fig. 5, Table S1).

The mean width was 9.2 μm for *Ganoderma,* 13 μm for *Cladosporium,* 15.4 μm for *Polythrincium,* 19.2 μm for *Alternaria,* and 20.4 μm for *Epicoccum* (Fig. 5).

Median spore height ranged from 11.3 μm in *Ganoderma* up to 27 μm in *Epicoccum*. The maximum height (81.8 μm) was recorded in *Epicoccum*, although its 95th percentile (34.6 μm) was substantially lower, suggesting that approximately 21 extreme values likely represent spore clumps that escaped the cleaning step. Height ranges spanned from 15.7 μm in *Ganoderma* to 70 μm in *Alternaria*.

Ganoderma and *Cladosporium* displayed the most similar width-to-height ratios, indicating that they have more circular spores. *Alternaria* exhibited the largest perimeter values across all metrics (median, 95th percentile, maximum), whereas *Ganoderma* consistently had the smallest. *Cladosporium* showed the highest number of upper-fence outliers (150), while *Polythrincium* had the lowest-fence outliers (224) (Fig. 5). A nearly twofold increase between the 95th percentile and maximum perimeter values in *Cladosporium* and *Epicoccum* likely reflects

Table 3
Spore season characteristics of individual fungal spore types during the study year, based on data collected with the POMO and BURK samplers.

Sampler	Spore type	ASIn_all	ASIn_ com	% of total	Ratio	Daily mean	Peak value	Peak date	High days
POMO	*Alternaria*	11,059	4539	14.1	1.21	64	742	201	32
	Cladosporium	27,519	11,521	35.1	0.09	160	1306	176	1
	Epicoccum	17,162	7053	21.9	2.12	100	864	282	58
	Ganoderma	495	204	0.6	0.01	3	17	227	0
	Polythrincium	22,112	9022	28.2	3.43	129	603	236	76
	Total	78,347	32,340		0.21				167
BURK	*Alternaria*	4050	3742	2.3	0.82	24	267	201	11
	Cladosporium	138,636	124,592	79.5	10.81	806	3212	263	48
	Epicoccum	3817	3330	2.2	0.47	22	216	282	4
	Ganoderma	25,026	22,281	14.4	109.22	146	565	243	94
	Polythrincium	2923	2627	1.7	0.29	17	86	236	0
	Total	174,452	156,571		4.84				157

ASIn – Annual Spore Integral (spore*day/m^3), *_all* – all days available, *ASIn _com* – days with samples from both monitors; *total* – summed concentration of the 5 selected spore types, Ratio – capture ratio between POMO and BURK on common days; *Daily mean* – mean daily spore concentration (spores/m^3); *Peak value* – maximum daily spore concentration (spores/m^3); *Peak date* (*DOY*) – day of the year from 1 January; *High days* – the number of days when spore concentration reached or exceeded the threshold value (1000 spores/m^3 for *Cladosporium*, and 100 spores/m^3 for all other spore types).

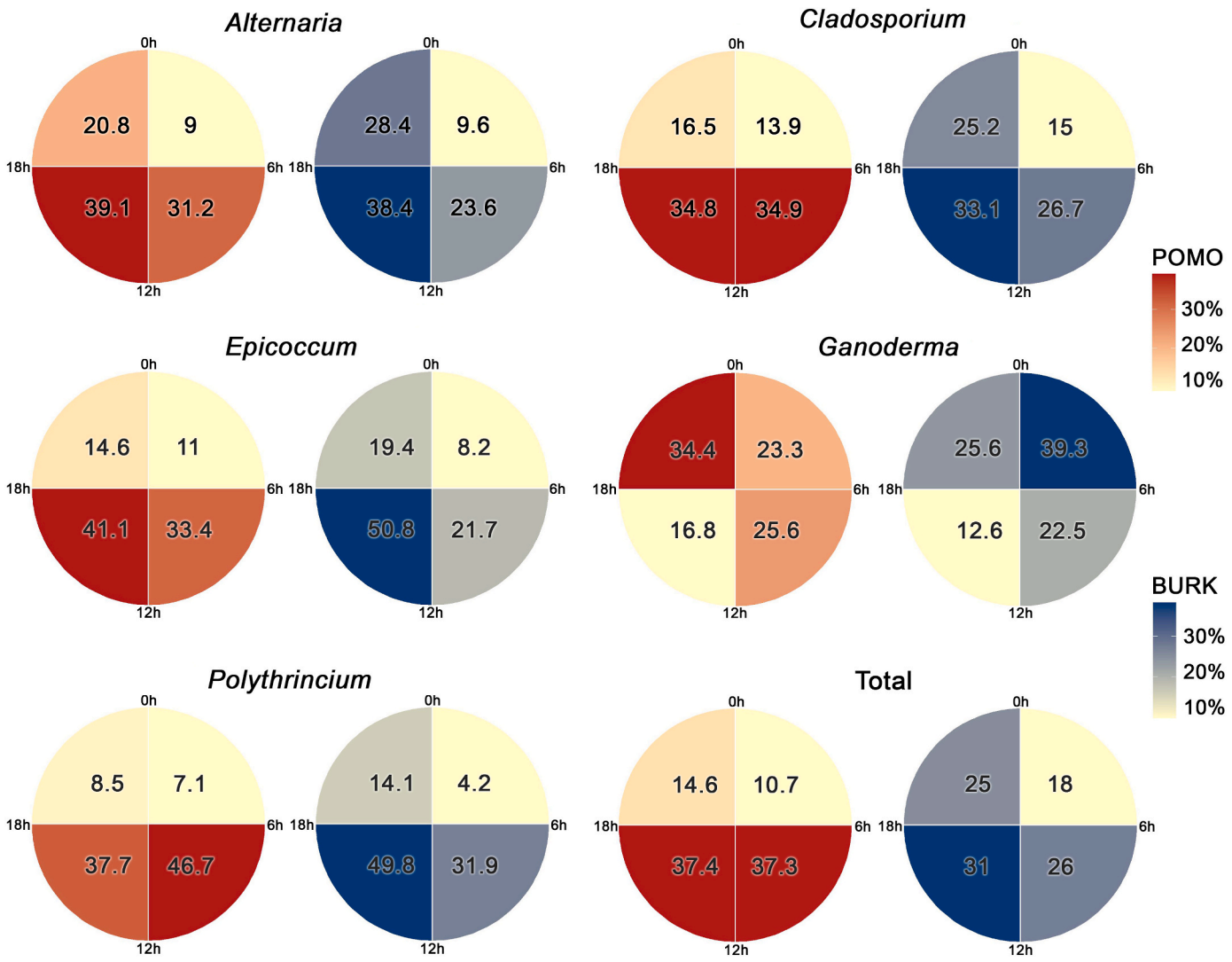

Fig. 2. Diurnal variation (%) in individual fungal spore types and total (summed) concentrations recorded by the POMO and BURK samplers.

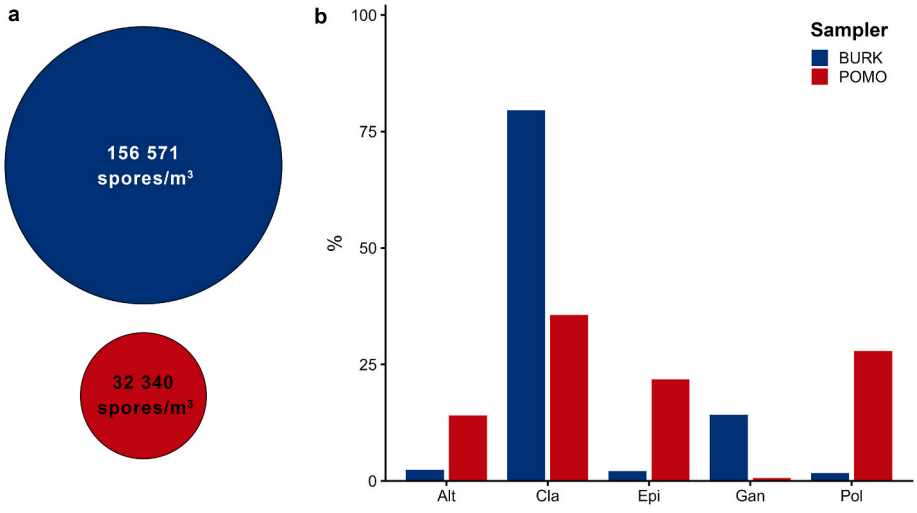

Fig. 3. Relative abundance of fungal spores (%) shown as (a) total concentration and (b) individual concentrations of each spore type (Alt – *Alternaria*, Cla – *Cladosporium*, Epi – *Epicoccum*, Gan – *Ganoderma*, Pol – *Polythrincium*) collected with the BURK and POMO samplers.

instances where two or more spores were adjacent.

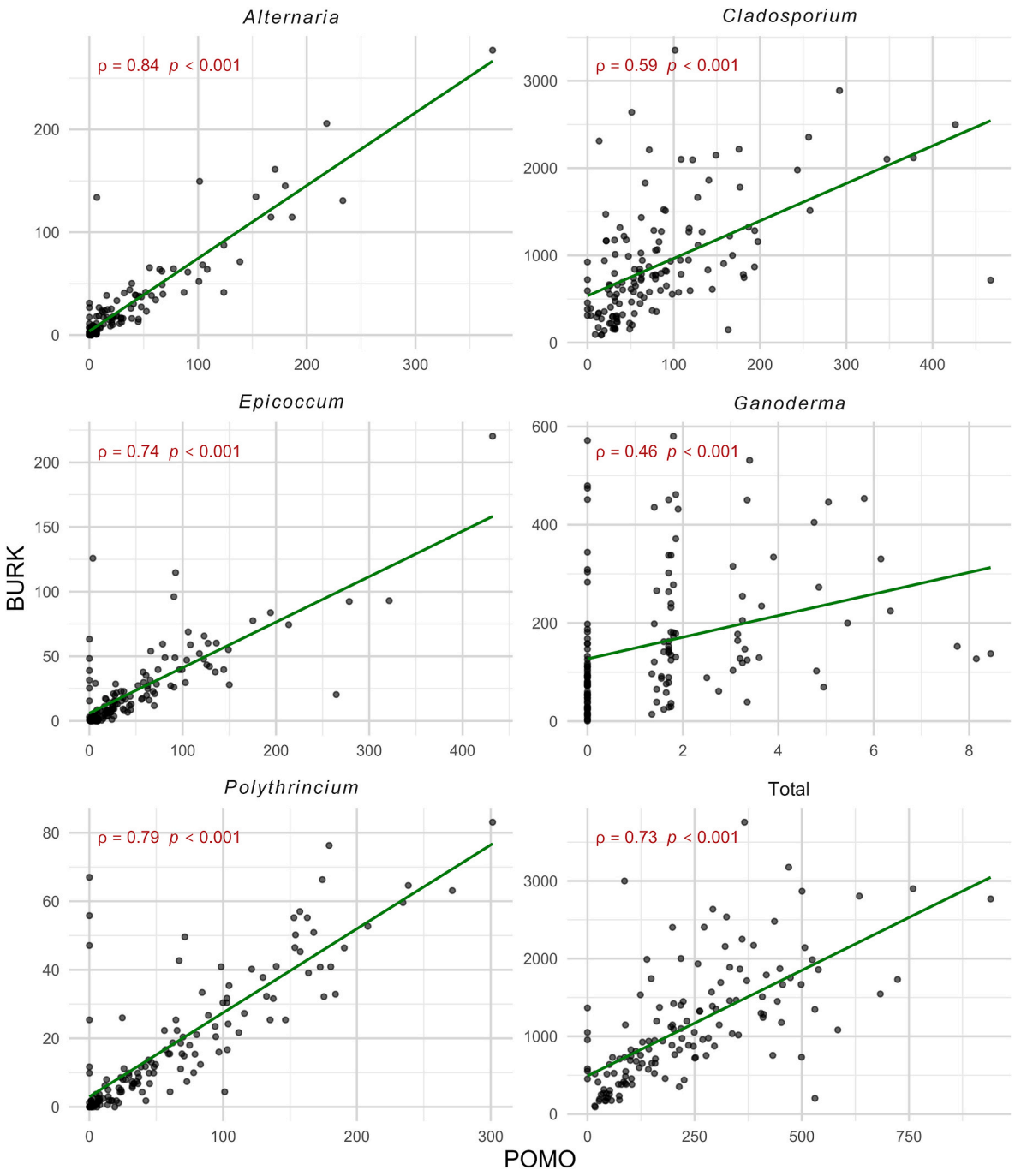

Fig. 4. Spearman correlation plots comparing spore concentrations measured by the POMO (x-axis) and BURK (y-axis) samplers, expressed as spores/m^3, for five fungal spore types and total (summed) daily concentrations.

3.3. Influence of meteorological parameters on fungal spore concentrations and monitors' capture efficiency

Redundancy analysis (RDA) revealed that meteorological variables significantly influenced the variation in spore concentrations captured by the two samplers. Air temperature was the primary factor associated with inter-sampler differences (partial $R^2 = 0.199$), followed by relative humidity (0.086) and rainfall (0.036), while air pressure and wind speed contributed only marginally (Fig. S5). The direction and length of vectors in the RDA biplot indicate positive relationships between individual meteorological parameters and variation in spore concentrations.

Overall correlations between spore concentrations and meteorological parameters were stronger for the BURK dataset (2-h resolution) than for the POMO dataset (3-h resolution), with an average difference of 0.136 in correlation strength. The taxa most affected by meteorological conditions were *Alternaria, Cladosporium,* and *Polythrincium*, all showing consistently higher correlations in BURK. Among all variables, air temperature exhibited the strongest positive correlations for both samplers, followed by ground temperature and sunshine duration. Relative humidity and rainfall were negatively associated with spore concentrations in nearly all taxa. *Ganoderma* was an exception, showing weak positive correlations with humidity and rainfall but a pronounced negative association with wind speed in BURK (Table 4).

Analysis of temperature ranges revealed a general increase in spore concentrations with rising temperatures, extending into the 30–35 °C range (Fig. 6). Below 15 °C, concentrations were generally low, but

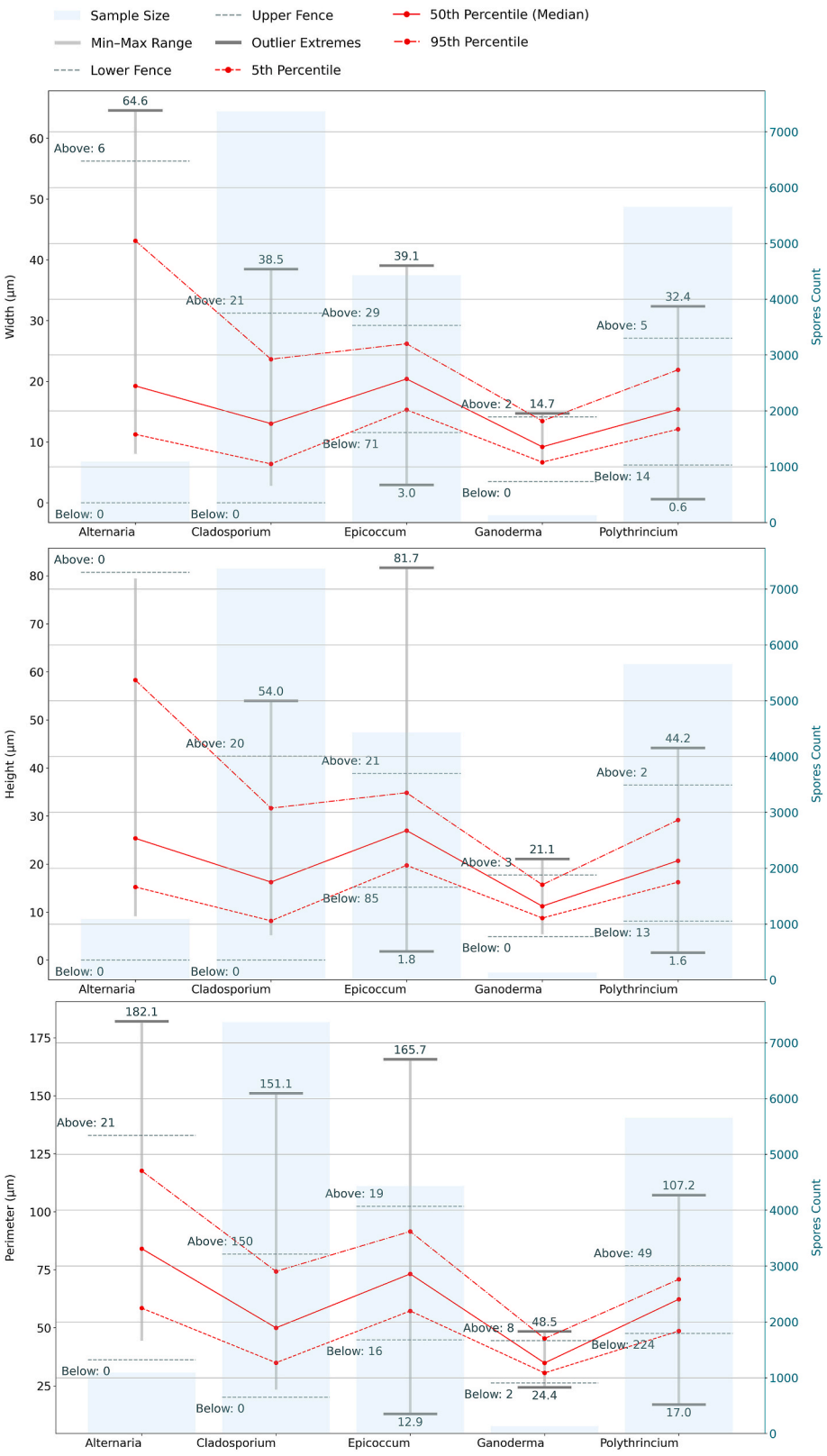

Fig. 5. Comparative summary of spore (a) width, (b) height, and (c) perimeter across five fungal spore types, captured by POMO.

Cladosporium (both devices), *Epicoccum* (POMO), and *Ganoderma* (BURK) still exhibited notable abundances even under <10 °C conditions. Both samplers displayed the most linear temperature-dependent increase for *Alternaria* and *Polythrincium*.

The Shapiro–Wilk test revealed significant non-normality for all spore types ($W = 0.358–0.793$, $p < 0.001$). Distributions were highly right-skewed ($\gamma_1 = 10–1032$).

Seasonal patterns differed among taxa. *Alternaria* exhibited the most pronounced seasonality, with a major peak in early August and a minor one in late September. *Polythrincium* showed a similar pattern with a

Table 4
Spearman's correlation coefficients between fungal spore concentrations collected with the POMO and BURK samplers and meteorological parameters. Significant trends are in bold.

Spore/Variable	AT	RH	R	AP	GT	WS	WD	SD
POMO								
Alternaria	**0.454*****	**−0.250***	**−0.211***	0.162	**0.400*****	−0.018	−0.053	**0.354*****
Cladosporium	**0.196***	−0.159	−0.156	0.175	0.140	−0.005	−0.077	**0.321****
Epicoccum	**0.200***	−0.119	−0.156	0.077	0.111	0.000	−0.001	**0.239***
Ganoderma	0.072	0.033	0.000	0.020	0.103	−0.068	−0.061	0.007
Polythrincium	**0.324****	−0.178	**−0.241***	0.107	**0.219***	−0.101	−0.053	**0.386*****
BURK								
Alternaria	**0.587*****	**−0.437*****	**−0.282****	0.178	**0.514*****	0.062	−0.088	**0.421*****
Cladosporium	**0.553*****	**−0.455*****	**−0.313****	0.164	**0.457*****	0.054	−0.189	**0.456*****
Epicoccum	**0.359*****	**−0.336*****	**−0.235***	0.107	**0.267****	0.090	−0.114	**0.376*****
Ganoderma	**0.247***	0.098	**−0.313****	0.142	**0.317****	**−0.469*****	**−0.194***	−0.083
Polythrincium	**0.460*****	**−0.420*****	**−0.285****	0.109	**0.338*****	0.038	−0.078	**0.483*****

AT-air temperature (°C); *RH* - relative humidity (%); *R* – rainfall (mm); *AP* - air pressure (hPa); *GT* - ground temperature (°C).
WS - wind speed (m/s); *WD* - wind direction (°); *SD* - sunshine duration (h); *p < 0.05; **p < 0.01; ***p < 0.001.

gradual rise from June to September. *Cladosporium* occurred throughout the entire sampling period with several moderate peaks, Epicoccum increased in late summer, and *Ganoderma* maintained moderate concentrations with occasional short-term peaks (Fig. S6).

4. Discussion

4.1. Fungal spore abundances

This study evaluated the capture efficiency of the POMO automatic monitor in comparison with the reference Hirst-type trap (BURK). Across the season (6 April–14 October 2024), 78,347 spores were recorded by POMO and 174,452 by BURK. The selected taxa represented a broad spectrum of particle sizes to test the performance of the POMO cascade impactor on environmentally and clinically important outdoor fungal pollution.

Cladosporium was the dominant spore type, consistent with reports from many sampled regions worldwide (Jiménez-Uribe et al., 2026; Martínez-Bracero et al., 2022; Ščevková et al., 2023; Simović et al., 2023) reaching levels capable of triggering allergy responses (Katotomichelakis et al., 2016). However, its dominance was substantially higher in BURK (79.5%) than in POMO (35.1%), reflecting more effective capture of small particles by Hirst-type traps. By contrast, POMO recorded much higher concentrations of *Epicoccum* and *Polythrincium,* whose size and morphology resemble pollen grains – the primary target for which the instrument was designed (Buters et al., 2024).

Alternaria accounted for 14.1% of POMO and 2.3% of BURK counts, with more than twice as many high days in POMO. This difference likely stems from POMO's detection algorithm and the characteristic morphology of *Alternaria*, which facilitates automated recognition. BURK may underrepresent large spores due to differences in inlet design and airflow. Conversely, *Ganoderma* was strongly underestimated by POMO (0.6% vs. 14.4% in BURK), as its small basidiospores (<5 μm) fall below the effective capture range of the POMO cascade impactor.

4.2. Comparison of capture efficiency

POMO accurately separated fungal spores into "Fungus" and "*Alternaria*" categories, although genus-level identification still requires additional labelling. When comparing POMO to other automatic devices, WIBS effectively detects fluorescent fungal particles (Cheng et al., 2020; Markey et al., 2022). Additionally, Swisens Poleno performs well for *Alternaria* (Maya-Manzano et al., 2023b) and was laboratory tested, along with Plair Rapid-E+, for 10 other fungal genera (Bruffaerts et al., 2025).

Capture efficiency differed markedly by spore size. BURK was more effective for small spores (*Cladosporium, Ganoderma*), while POMO captured mid-sized spores (*Epicoccum, Polythrincium*) more efficiently. These findings align with known performance characteristics of Hirst-type traps (Frenz, 1999; Peel et al., 2014) and with previous observations that POMO and Poleno correlate best with particles >5 μm (Sauvageat et al., 2020). The cascade impactor design of POMO discards the smallest particles (Buters et al., 2024), which was confirmed by our size analysis and the large discrepancy between POMO and BURK for *Cladosporium* and *Ganoderma*. Algorithmic thresholds may further contribute to under-detection of small particles, a problem also reported for fluorescence-based instruments (Saari et al., 2014). Algorithm adjustments or size-specific scaling factors may improve compatibility with Hirst data. However, because Hirst traps have well-known biases and lack an official calibration standard, defining the "true" airborne concentration remains a challenge. Ongoing development of calibration protocols within the EU project BioAirMet may provide future solutions.

Correlation values obtained for *Alternaria* ($\rho = 0.84$) were comparable to previous POMO-Hirst pollen comparisons (Maya-Manzano et al. 2023). Nevertheless, both POMO and BURK may underestimate large *Alternaria* spores (>100 μm; Simon et al., 2009) that exceed their detection ranges. Lower correlations for *Polythrincium* and *Epicoccum* may reflect sampler airflow dynamics, especially during periods of extremely low or high concentrations when BURK measurement uncertainty increases (Adamov et al., 2021). Similar discrepancies were reported during the 2021 EUMETNET Autopollen campaign, where POMO captured more *Poaceae* pollen than Hirst traps (Maya-Manzano et al. 2023).

Both devices showed similar diurnal patterns. *Alternaria* and *Cladosporium* peaked between 12:00 and 18:00, coinciding with rising temperature, decreasing relative humidity, and increased turbulence, well-documented drivers of conidial release (Grinn-Gofroń and Strzelczak, 2009; O'Connor et al., 2014; Olsen et al., 2020). The negative relationship with relative humidity is consistent with easier detachment and suspension of spores on conidiophores, resulting in higher spore concentrations during the drier parts of the day (Abel Fernández et al., 2023). *Ganoderma* displayed the expected nocturnal pattern, with peaks around midnight, consistent with moisture-independent basidiospore release and UV avoidance (Ho and Nawawi, 1986; López-Vásquez et al., 2024).

4.3. Spore size distribution

Size variability was highest in *Alternaria* due to its diverse morphotypes and appendages, which influence shape and optical segmentation. Environmental humidity further affects spore swelling or desiccation, contributing to the wide range of observed values.

Cladosporium exhibited unexpectedly broad size distribution, likely due to frequent clumping despite rigorous cleaning prior to analysis. Many particles exceeded plausible dimensions for single spores. This is

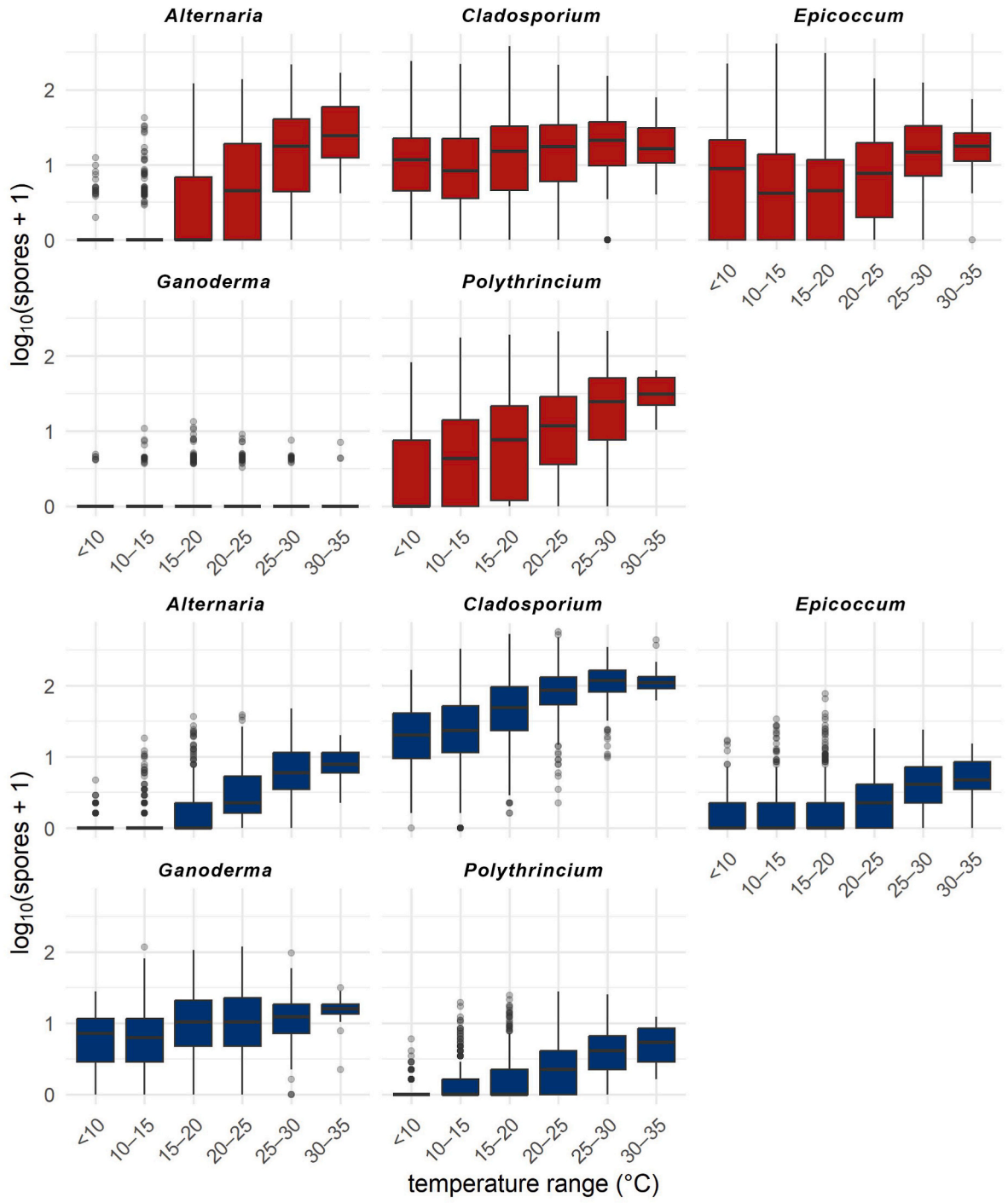

Fig. 6. Distribution of spore concentrations across temperature ranges recorded by the POMO (red, top) and BURK (blue, bottom) samplers during the study period. (For interpretation of the references to colour in this figure legend, the reader is referred to the Web version of this article.)

consistent with the high morphological variability typical of ascomycetous conidia (Jadhav et al., 2011; Hafizi et al., 2013; Mugao, 2023).

Epicoccum and *Polythrincium* showed comparatively narrow size ranges, reflecting their regular, mostly spherical shape. Interpretation of *Ganoderma* size patterns remains limited due to the small sample size (129 spores), although basidiospores are generally more uniform. Segmented image measurements may underestimate true dimensions; therefore, fences were applied to filter abnormal values.

4.4. Influence of meteorological parameters on fungal spore concentrations

Correlation strengths were generally higher for BURK than for POMO, because POMO is temperature-controlled and has a much higher intake volume, making it less sensitive to external fluctuations. Similar findings were reported by González-Alonso et al. (2023).

RDA indicated that meteorological factors explained over 30% of the variation between the two devices. Air temperature and relative humidity were the primary drivers, closely matching findings from the EUMETNET Autopollen campaign. Temperature and sunshine were

positively associated with spore concentrations, whereas humidity and rainfall showed negative correlations, consistent with the dry-spore release strategy of most analysed taxa (Grinn-Gofroń et al., 2018; Ianovici, 2016). Only *Ganoderma* showed weak correlations in POMO and a pronounced negative association with wind speed in BURK, likely due to displacement of small basidiospores at higher wind velocities.

Spore concentrations increased with temperature across all taxa, including 30–35 °C range, except for *Cladosporium*, which peaked around 25–30 °C. Temperature is considered as a strong positive factor influencing airborne fungal pollution (Grinn-Gofroń et al., 2011), although its effects on sporulation may vary across regions and taxa. While several studies report reduced sporulation above 27 °C (Damialis et al., 2015; Grinn-Gofroń et al., 2018; Martínez-Bracero et al., 2020), others show increases up to >31 °C (Sánchez Espinosa et al., 2024). Considering that sporulation enhances resilience to environmental stress, increased airborne spore loads during more frequent heat events may be expected, highlighting the need to account for heat-driven changes in bioaerosol exposure under future climate scenarios.

4.5. Fungal spore temporal patterns

Both devices showed comparable seasonal dynamics, with low counts in spring and maxima during late summer and early autumn (August–September). Although only one year of measurements is available, the timing broadly agrees with patterns from Central European regions such as Rzeszów, Warsaw, and Bratislava (Anees-Hill et al., 2022) showing the monitoring potential of POMO for fungal spores. However, our ground-level setup surrounded by buildings likely amplified local signals and reduced comparability with rooftop monitoring, which may explain the less pronounced seasonal pattern.

Polythrincium reached exceptionally high levels, far exceeding previously reported values. This strongly suggests a local infection source at the sampling site, consistent with its role as a pathogen of *Trifolium prantense* (red clover) (Simon et al., 2009).

Epicoccum concentrations peaked late in the season, consistent with findings from Slovakia (Žilka et al., 2024), England (Sadyś et al., 2016), and Poland (Grinn-Gofroń and Mika, 2008). *Alternaria* dynamics should be interpreted in the context of local microclimate, sampler height, and nearby vegetation or pollution sources, as highlighted by Plaza et al. (2025).

5. Conclusions

The aim of this study was to test the potential to use the POMO as an airborne fungal spore monitor. Overall, the device demonstrated satisfactory performance. The findings suggest that automatic POMO devices can effectively detect environmentally relevant airborne fungal spores, particularly medium- and large-sized particles such as *Alternaria, Epicoccum* and *Polythrinicum*. This shows strong potential for agricultural, medical, and forestry applications, as it can detect even low spore concentrations that may still initiate plant disease or contribute to allergy development. The near real-time availability of data represents an additional major advantage, supporting the development of early warning systems and enabling rapid responses during the critical first hours to days after disease onset.

However, compared with the Hirst-type reference, POMO showed lower efficiency in detecting small spores, likely due to both sampling mechanics and classification constraints. As *Ganoderma* and *Cladosporium* are important indicators of plant- or wood-related diseases, their underestimation highlights the continued need for Hirst-type monitoring until the determination and application of type-specific correction factors for small spores.

Sampling efficiency is likely to vary among bioaerosols with differing physical and optical properties; thus, further technological refinement and broader validation across the full particle-size spectrum are needed.

Finally, although the influence of meteorological parameters on airborne spores is well established, the observed increase in spore concentrations even at temperatures between 30 °C and 35 °C suggests possible thermal adaptation. Such shifts may increase the risk of fungal plant diseases and allergic responses under future climatic conditions.

CRediT authorship contribution statement

Matúš Žilka: Writing – review & editing, Writing – original draft, Visualization, Validation, Software, Methodology, Formal analysis, Data curation. **Samer Alashhab:** Writing – review & editing, Writing – original draft, Methodology, Formal analysis, Data curation. **Jana Ščevková:** Writing – review & editing. **Carsten B. Schmidt-Weber:** Writing – review & editing. **Inga Wessels:** Writing – review & editing, Supervision, Funding acquisition. **Jeroen Buters:** Writing – review & editing, Supervision, Funding acquisition. **Mónica González-Alonso:** Writing – review & editing, Writing – original draft, Visualization, Supervision, Methodology, Formal analysis, Data curation, Conceptualization.

Funding

This work was supported by the European Union through the NextGenerationEU initiative under the Recovery and Resilience Plan of the Slovak Republic (project no. 09I03-03-V05-00012, UK/3011/2024), Grant Agency VEGA (Bratislava), Grant No. 1/0180/22.

Declaration of competing interest

The authors declare the following financial interests/personal relationships which may be considered as potential competing interests: Matus Zilka reports financial support was provided by European Union through the NextGenerationEU initiative under the Recovery and Resilience Plan of the Slovak Republic (project no. 09I03-03-V05-00012, UK/3011/2024), Grant Agency VEGA (Bratislava), Grant No. 1/0180/22. If there are other authors, they declare that they have no known competing financial interests or personal relationships that could have appeared to influence the work reported in this paper.

Acknowledgements

We would like to thank Dr. Wessels and Prof. Dr. Buters for welcoming Matus into the group and facilitating the completion of the project.

Appendix A. Supplementary data

Supplementary data to this article can be found online at https://doi.org/10.1016/j.envpol.2026.128148.

Data availability

Data and code are published at the Zenodo repository, information is in the manuscript

References

Abel-Fernández, E., Martínez, M.J., Galán, T., Pineda, F., 2023. Going over fungal allergy: Alternaria Alternata and its allergens. J. Fungi 9 (5), 582. https://doi.org/10.3390/jof9050582.

Adamov, S., Lemonis, N., Clot, B., Crouzy, B., Gehrig, R., Graber, M.-J., Sallin, C., Tummon, F., 2021. On the measurement uncertainty of Hirst-type volumetric pollen and spore samplers. Aerobiologia 40. https://doi.org/10.1007/s10453-021-09724-5.

Anees-Hill, S., Douglas, P., Pashley, C.H., Hansell, A., Marczylo, E.L., 2022. A systematic review of outdoor airborne fungal spore seasonality across Europe and the implications for health. Sci. Total Environ. 818, 151716. https://doi.org/10.1016/j.scitotenv.2021.151716.

Bruffaerts, N., Graf, E., Matavulj, P., Tiwari, A., Pyrri, I., Zeder, Y., Erb, S., Plaza, M., Dietler, S., Bendinelli, T., D'hooge, E., Sikoparija, B., 2025. Advancing automated

identification of airborne fungal spores: guidelines for cultivation and reference dataset creation. Aerobiologia 41, 505–525. https://doi.org/10.1007/s10453-025-09864-y.

Buters, J., Clot, B., Galán, C., Gehrig, R., Gilge, S., Hentges, F., O'Connor, D., Sikoparija, B., Skjoth, C., Tummon, F., Adams-Groom, B., Antunes, C.M., Bruffaerts, N., Çelenk, S., Crouzy, B., Guillaud, G., Hajkova, L., Seliger, A.K., Oliver, G., Ribeiro, H., Rodinkova, V., Saarto, A., Sauliene, I., Sozinova, O., Stjepanovic, B., 2024. Automatic detection of airborne pollen: an overview. Aerobiologia 40, 13–37. https://doi.org/10.1007/s10453-022-09750-x.

Buters, J.T.M., Antunes, C., Galveias, A., Bergmann, K.C., Thibaudon, M., Galán, C., Schmidt-Weber, C., Oteros, J., 2018. Pollen and spore monitoring in the world. Clin. Transl. Allergy 8, 9. https://doi.org/10.1186/s13601-018-0197-8.

Cheng, B., Yue, S., Hu, W., Ren, L., Deng, J., Wu, L., Fu, P., 2020. Summertime fluorescent bioaerosol particles in the coastal megacity Tianjin, North China. Sci. Total Environ. 723, 137966. https://doi.org/10.1016/j.scitotenv.2020.137966.

D'Amato, G., Cecchi, L., Bonini, S., Nunes, C., Annesi-Maesano, I., Behrendt, H., Liccardi, G., Popov, T., van Cauwenberge, P., 2007. Allergenic pollen and pollen allergy in Europe. Allergy 62, 976–990. https://doi.org/10.1111/j.1398-9995.2007.01393.x.

Damialis, A., Mohammad, A.B., Halley, J.M., Gange, A.C., 2015. Fungi in a changing world: growth rates will be elevated, but spore production may decrease in future climates. Int. J. Biometeorol. 59, 1157–1167. https://doi.org/10.1007/s00484-014-0927-0.

Després, V.R., Huffman, J.A., Burrows, S.M., Hoose, C., Safatov, A.S., Buryak, G., Fröhlich-Nowoisky, J., Elbert, W., Andreae, M.O., Pöschl, U., Jaenicke, R., 2012. Primary biological aerosol particles in the atmosphere: a review. Tellus Ser. B Chem. Phys. Meteorol. B 64, 15598. https://doi.org/10.3402/tellusb.v64i0.15598.

Doehlemann, G., Ökmen, B., Zhu, W., Sharon, A., 2017. Plant pathogenic fungi. Microbiol. Spectr. 5. https://doi.org/10.1128/microbiolspec.FUNK-0023-2016.

Frenz, D.A., 1999. Comparing pollen and spore counts collected with the Rotorod Sampler and Burkard spore trap. Ann. Allergy Asthma Immunol. 83, 341–349. https://doi.org/10.1016/S1081-1206(10)62828-1.

Fröhlich, J., Kampf, C.J., Weber, B., Huffman, J.A., Pöhlker, C., Andreae, M.O., Lang-Yona, N., Burrows, S.M., Gunthe, S.S., Elbert, W., Su, H., Hoor, P., Thines, E., Hoffmann, T., Després, V.R., Pöschl, U., 2016. Bioaerosols in the Earth system: climate, health, and ecosystem interactions. Atmos. Res. 182, 346–376. https://doi.org/10.1016/j.atmosres.2016.07.018.

Galán, C., Smith, M., Thibaudon, M., Frenguelli, G., Oteros, J., Gehrig, R., Berger, U., Clot, B., Brandao, R., EAS QC Working Group, 2014. Pollen monitoring: minimum requirements and reproducibility of analysis. Aerobiologia 30, 385–395. https://doi.org/10.1007/s10453-014-9335-5.

González-Alonso, M., Boldeanu, M., Koritnik, T., Gonçalves, J., Belzner, L., Stemmler, T., Gebauer, R., Grewling, Ł., Tummon, F., Maya-Manzano, J.M., Ariño, A.H., Schmidt-Weber, C., Buters, J., 2023. *Alternaria* spore exposure in Bavaria, Germany, measured using artificial intelligence algorithms in a network of BAA500 automatic pollen monitors. Sci. Total Environ. 861, 160180. https://doi.org/10.1016/j.scitotenv.2022.160180.

Grinn-Gofroń, A., Bosiacka, B., 2015. Effects of meteorological factors on the composition of selected fungal spores in the air. Aerobiologia 31, 63–72. https://doi.org/10.1007/s10453-014-9347-1.

Grinn-Gofroń, A., Bosiacka, B., Bednarz, A., Wolski, T., 2018. A comparative study of hourly and daily relationships between selected meteorological parameters and airborne fungal spore composition. Aerobiologia 34, 45–54. https://doi.org/10.1007/s10453-017-9493-3.

Grinn-Gofroń, A., Mika, A., 2008. Selected airborne allergenic fungal spores and meteorological factors in Szczecin, Poland, 2004–2006. Aerobiologia 2, 89–97. https://doi.org/10.1007/s10453-008-9088-0.

Grinn-Gofroń, A., Strzelczak, A., 2009. Hourly predictive artificial neural network and multivariate regression tree models of Alternaria and Cladosporium spore concentrations in Szczecin (Poland). Int. J. Biometeorol. 53, 555–562. https://doi.org/10.1007/s00484-009-0243-2.

Grinn-Gofroń, A., Strzelczak, A., Wolski, T., 2011. The relationships between air pollutants, meteorological parameters and concentration of airborne fungal spores. Environ. Pollut. 159, 602–608. https://doi.org/10.1016/j.envpol.2010.10.002.

Hafizi, R., Salleh, B., Latiffah, Z., 2013. Morphological and molecular characterization of Fusarium. solani and F. oxysporum associated with crown disease of oil palm. Braz. J. Microbiol. 44, 959–968. https://doi.org/10.1590/s1517-83822013000300047.

Hirst, J.M., 1952. An automatic volumetric spore trap. Ann. Appl. Biol. 39, 257–265. https://doi.org/10.1111/j.1744-7348.1952.tb00904.x.

Ho, Y.W., Nawawi, A., 1986. Diurnal periodicity of spore discharge in Ganoderma boninense Pat. from Oil palm inMalaysia. Pertanika 9 (2), 147–150.

Ianovici, N., 2016. Atmospheric concentrations of selected allergenic fungal spores in relation to some meteorological factors, in Timişoara (Romania). Aerobiologia 1, 139–156. https://doi.org/10.1007/s10453-016-9427-5.

Idris, A.S., Kushairi, A., Ismail, S., Ariffin, D., 2004. Selection for partial resistance in oil palm progenies to Ganoderma basal stem rot. Journal of Oil Palm Research.

Jadhav, B.M., Perane*, R.R., Kale, A.A., Pawar, N.B., 2011. Morphological, pathological and molecular variability among Alternaria macrospora isolates causing leaf blight of cotton. Indian Phytopathol. 64, 254–257.

Jiménez-Uribe, D.A., Acevedo-Barrios, R., Rubiano-Labrador, C., Cariñanos, P., 2026. Relationship of airborne fungal spores to epidemiological data on respiratory disease: a systematic review. Aerobiologia 42, 11. https://doi.org/10.1007/s10453-025-09890-w.

Jin, M., Yang, C., Wang, Y., Wei, L., Osei, R., 2023. Isolation and identification of Epicoccum nigrum as the causal agent of brown spot disease in Solanum tuberosum in China. Plant Pathol. 72, 829–838. https://doi.org/10.1111/ppa.13696.

Kasprzyk, I., Worek, M., 2006. Airborne fungal spores in urban and rural environments in Poland. Aerobiologia 22, 169–176. https://doi.org/10.1007/s10453-006-9029-8.

Katotomichelakis, M., Nikolaidis, C., Makris, M., Proimos, E., Aggelides, X., Constantinidis, T.C., Papadakis, C.E., Danielides, V., 2016. Alternaria and Cladosporium calendar of Western Thrace: relationship with allergic rhinitis symptoms. Laryngoscope 126, E51–E56. https://doi.org/10.1002/lary.25594.

Kukreja, N., Sridhara, S., Singh, B.P., Arora, N., 2008. Effect of proteolytic activity of Epicoccum purpurascens major allergen, Epi p 1 in allergic inflammation. Clin. Exp. Immunol. 154, 162–171. https://doi.org/10.1111/j.1365-2249.2008.03762.x.

Lacey, M.E., West, J.S., 2006. The Air Spora: a Manual for Catching and Identifying Airborne Biological Particles. Springer, Dordrecht.

Li, D.-W., Magyar, D., Kendrick, B., 2023. Color Atlas of Fungal Spores. A Laboratory Identification Guide.

López-Vásquez, J.M., Castillo, S.Y., Zúñiga, L.F., Sarria, G.A., Morales-Rodríguez, A., 2024. Temporal dynamics of airborne concentrations of ganoderma basidiospores and their relationship with environmental conditions in oil palm (Elaeis guineensis). J. Fungi 10, 479. https://doi.org/10.3390/jof10070479.

Lucas, R.W., Bunderson, L., 2024. A review of pollen counting networks: from the nineteenth century into the twenty-first century. Curr. Allergy Asthma Rep. 24, 1–9. https://doi.org/10.1007/s11882-023-01119-5.

Markey, E., Hourihane Clancy, J., Martínez-Bracero, M., Neeson, F., Sarda-Estève, R., Baisnée, D., McGillicuddy, E.J., Sewell, G., O'Connor, D.J., 2022. A modified spectroscopic approach for the real-time detection of pollen and fungal spores at a semi-urban site using the WIBS-4+, part I. Sensors 22, 8747. https://doi.org/10.3390/s22228747.

Martínez-Bracero, M., González-Fernández, E., Wójcik, M., Alcázar, P., Fernández-González, M., Kasprzyk, I., Rajo, F.J., Galán, C., 2020. Airborne fungal phytopathological spore assessment in three European vineyards from different bioclimatic areas. Aerobiologia 36, 1–15. https://doi.org/10.1007/s10453-020-09664-6.

Martínez-Bracero, M., Markey, E., Clancy, J.H., McGillicuddy, E.J., Sewell, G., O'Connor, D.J., 2022. Airborne fungal spore review, new advances and automatisation. Atmosphere 13, 308. https://doi.org/10.3390/atmos13020308.

Maya-Manzano, J.M., Tummon, F., Abt, R., Allan, N., Bunderson, L., Clot, B., Crouzy, B., Daunys, G., Erb, S., Gonzalez-Alonso, M., Graf, E., Grewling, Ł., Haus, J., Kadantsev, E., Kawashima, S., Martinez-Bracero, M., Matavulj, P., Mills, S., Niederberger, E., Lieberherr, G., Lucas, R.W., O'Connor, D.J., Oteros, J., Palamarchuk, J., Pope, F.D., Rojo, J., Šaulienė, I., Schäfer, S., Schmidt-Weber, C.B., Schnitzler, M., Šikoparija, B., Skjøth, C.A., Sofiev, M., Stemmler, T., Triviño, M., Zeder, Y., Buters, J., 2023a. Towards European automatic bioaerosol monitoring: Comparison of 9 automatic pollen observational instruments with classic Hirst-type traps. Sci. Total Environ. 866, 161220. https://doi.org/10.1016/j.scitotenv.2022.161220.

Maya-Manzano, J.M., Tummon, F., Abt, R., Allan, N., Bunderson, L., Clot, B., Crouzy, B., Daunys, G., Erb, S., Gonzalez-Alonso, M., Graf, E., Grewling, Ł., Haus, J., Kadantsev, E., Kawashima, S., Martinez-Bracero, M., Matavulj, P., Mills, S., Niederberger, E., Lieberherr, G., Lucas, R.W., O'Connor, D.J., Oteros, J., Palamarchuk, J., Pope, F.D., Rojo, J., Šaulienė, I., Schäfer, S., Schmidt-Weber, C.B., Schnitzler, M., Šikoparija, B., Skjøth, C.A., Sofiev, M., Stemmler, T., Triviño, M., Zeder, Y., Buters, J., 2023b. Towards European automatic bioaerosol monitoring: Comparison of 9 automatic pollen observational instruments with classic Hirst-type traps. Sci. Total Environ. 866, 161220. https://doi.org/10.1016/j.scitotenv.2022.161220.

Miki, K., Kawashima, S., Clot, B., Nakamura, K., 2019. Comparative efficiency of airborne pollen concentration evaluation in two pollen sampler designs related to impaction and changes in internal wind speed. Atmos. Environ. 203, 18–27. https://doi.org/10.1016/j.atmosenv.2019.01.039.

Mugao, L., 2023. Morphological and molecular variability of Alternaria solani and Phytophthora infestans causing tomato blights. Internet J. Microbiol., 8951351 https://doi.org/10.1155/2023/8951351, 2023.

O'Connor, D.J., Sadyś, M., Skjøth, C.A., Healy, D.A., Kennedy, R., Sodeau, J.R., 2014. Atmospheric concentrations of Alternaria, Cladosporium, Ganoderma and Didymella spores monitored in Cork (Ireland) and Worcester (England) during the summer of 2010. Aerobiologia 30, 397–411. https://doi.org/10.1007/s10453-014-9337-3.

Oliveira, M., Ribeiro, H., Delgado, L., Fonseca, J., Castel-Branco, M.G., Abreu, I., 2010. Outdoor allergenic fungal spores: comparison between an urban and a rural area in northern Portugal. J Investig. Allergol. Clin. Immunol. 20, 117–128.

Olsen, Y., Skjøth, C., Hertel, O., Rasmussen, K., Sigsgaard, T., Gosewinkel, U., 2020. Airborne Cladosporium and Alternaria spore concentrations through 26 years in Copenhagen, Denmark. Aerobiologia 36. https://doi.org/10.1007/s10453-019-09618-7.

Oteros, J., Pusch, G., Weichenmeier, I., Heimann, U., Möller, R., Röseler, S., Traidl-Hoffmann, C., Schmidt-Weber, C., Buters, J.T.M., 2015. Automatic and online pollen monitoring. Int. Arch. Allergy Immunol. 167, 158–166. https://doi.org/10.1159/000436968.

Oteros, J., Weber, A., Kutzora, S., Rojo, J., Heinze, S., Herr, C., Gebauer, R., Schmidt-Weber, C.B., Buters, J.T.M., 2020. An operational robotic pollen monitoring network based on automatic image recognition. Environ. Res. 191, 110031. https://doi.org/10.1016/j.envres.2020.110031.

Peel, R.G., Kennedy, R., Smith, M., Hertel, O., 2014. Relative efficiencies of the Burkard 7-Day, Rotorod and Burkard Personal Samplers for Poaceae and Urticaceae pollen under field conditions. Ann. Agric. Environ. Med. 21, 745–752. https://doi.org/10.5604/12321966.1129927.

Plaza, M.P., Oteros, J., Leier-Wirtz, V., Kolek, F., Menzel, A., Buters, J.T.M., Traidl-Hoffmann, C., Damialis, A., 2025. A multi-scale analysis of airborne *Alternaria* spore

dispersal: influence of meteorology, land cover and air pollution. Agric. For. Meteorol. 372, 110716. https://doi.org/10.1016/j.agrformet.2025.110716.
Saari, S., Reponen, T., Keskinen, J., 2014. Performance of two fluorescence-based real-time bioaerosol detectors: BioScout vs. UVAPS. Aerosol. Sci. Technol. 48, 371–378. https://doi.org/10.1080/02786826.2013.877579.
Sadyś, M., Adams-Groom, B., Herbert, R.J., Kennedy, R., 2016. Comparisons of fungal spore distributions using air sampling at Worcester, England (2006–2010). Aerobiologia 32, 619–634. https://doi.org/10.1007/s10453-016-9436-4.
Sánchez Espinosa, K.C., Aira, M.J., Fernández-González, M., Rodríguez-Rajo, F.J., 2024. Airborne Alternaria spores: 70 annual records in Northwestern Spain. J. Fungi 10, 681. https://doi.org/10.3390/jof10100681.
Santarpia, J.L., 2016. Bioaerosols in the environment: populations, measurement and processes. In: Salem, H., Katz, S.A. (Eds.), Aerobiology: the Toxicology of Airborne Pathogens and Toxins. The Royal Society of Chemistry. https://doi.org/10.1039/9781849737913-00219.
Sauvageat, E., Zeder, Y., Auderset, K., Calpini, B., Clot, B., Crouzy, B., Konzelmann, T., Lieberherr, G., Tummon, F., Vasilatou, K., 2020. Real-time pollen monitoring using digital holography. Atmos. Meas. Tech. 13, 1539–1550. https://doi.org/10.5194/amt-13-1539-2020.
Ščevková, J., Vašková, Z., Dušička, J., Žilka, M., Zvaríková, M., 2023. Co-occurrence of airborne biological and anthropogenic pollutants in the central European urban ecosystem. Environ. Sci. Pollut. Res. Int. 30, 26523–26534. https://doi.org/10.1007/s11356-022-24048-8.
Schmey, T., Tominello-Ramirez, C.S., Brune, C., Stam, R., 2024. Alternaria diseases on potato and tomato. Mol. Plant Pathol. 25, e13435. https://doi.org/10.1111/mpp.13435.
Sikoparija, B., Galán, C., Smith, M., Abramidze, T., Adams-Groom, B., Albertini, R., Anelli, P., Bastl, K., Bigagli, V., Bonini, M., Bócsi, E., Bucher, E., Caeiro, E., Celenk, S., Cerovac, Ž., Chłopek, K., Cislaghi, G., Clot, B., Cortonesi, B., Cristofori, A., Dahl, A., Della Bella, V., Dupuy, N., Dušička, J., Ferro, R., Flori, C., Graber, M.J., Hrastovćak, S., Ianovici, N., Józsa, E., Kasprzyk, I., Kmenta, M., Kofler, V., Magyar, D., Mányoki, G., Maya Manzano, J.M., Myszkowska, D., Nowak, M., Oliver, G., Paganoni, B., Palamarchuk, O., Parati, S., Pashley, C., Pini, A., Piotrowska, K., Prentović, M., Rachoud, A.M., Radišić, P., Rapp Benito, A., Rodinkova, V., Russo, M., Sallin, C., Satchwell, J., Sindt, C., Smith, M., Szymanska, A., Šaulienė, I., Ščevková, J., Šikoparija, B., Tassan Mazzocco, F., Testoni, C., Tomičić Žabčić, V., Udvardy, O., Ugolotti, M., Vadassy, R., Vannini, J., Vecenaj, A., Velasco-Jiménez, M.J., Verardo, P., Viola, M.C., Vuillemin, F., Zemmer, F., EAS QC Working Group, 2017. Pollen-monitoring: between analyst proficiency testing. Aerobiologia 33, 191–199. https://doi.org/10.1007/s10453-016-9461-3.
Simon, U.K., Groenewald, J.Z., Crous, P.W., 2009. Cymadothea trifolii, an obligate biotrophic leaf parasite of Trifolium, belongs to Mycosphaerellaceae as shown by nuclear ribosomal DNA analyses. Persoonia 22, 49–55. https://doi.org/10.3767/003158509X425350.
Simović, I., Matavulj, P., Šikoparija, B., 2023. Manual and automatic quantification of airborne fungal spores during wheat harvest period. Aerobiologia 39, 227–239. https://doi.org/10.1007/s10453-023-09788-5.
Smith, E.G., 2000. Sampling & Identifying Allergenic Pollens & Molds, 1 edition. Blewstone Press, San Antonio, Tex.
Straumfors, A., Mundra, S., Foss, O.A.H., Mollerup, S.K., Kauserud, H., 2021. The airborne mycobiome and associations with mycotoxins and inflammatory markers in the Norwegian grain industry. Sci. Rep. 11, 9357. https://doi.org/10.1038/s41598-021-88252-1.
Suarez-Suarez, M., Maya-Manzano, J.M., Clot, B., Graber, M.-J., Sallin, C., Tummon, F., Buters, J., 2023. Accuracy of a hand-held resistance-free flowmeters for flow adjustments of Hirst-Type pollen traps. Aerobiologia 39, 143–148. https://doi.org/10.1007/s10453-023-09782-x.
Taguiam, J.D., Evallo, E., Balendres, M.A., 2021. Epicoccum species: ubiquitous plant pathogens and effective biological control agents. Eur. J. Plant Pathol. 159, 713–725. https://doi.org/10.1007/s10658-021-02207-w.
Triviño, M.M., Maya-Manzano, J.M., Tummon, F., Clot, B., Grewling, Ł., Schmidt-Weber, C., Buters, J., 2023. Variability between Hirst-type pollen traps is reduced by resistance-free flow adjustment. Aerobiologia 39, 257–273. https://doi.org/10.1007/s10453-023-09790-x.
Tukey, J.W., John, W., 1977. Exploratory Data Analysis. Addison-Wesley Pub. Co, Reading, Mass.
Williams, S.L., Toda, M., Chiller, T., Brunkard, J.M., Litvintseva, A.P., 2024. Effects of climate change on fungal infections. PLoS Pathog. 20, e1012219. https://doi.org/10.1371/journal.ppat.1012219.
Zhao, X., Liu, Y., Huang, Z., Li, G., Zhang, Z., He, X., Du, H., Wang, M., Li, Z., 2024. Early diagnosis of Cladosporium fulvum in greenhouse tomato plants based on visible/near-infrared (VIS/NIR) and near-infrared (NIR) data fusion. Sci. Rep. 14, 20176. https://doi.org/10.1038/s41598-024-71220-w.
Žilka, M., Hrabovský, M., Dušička, J., Zahradníková, E., Gahurova, D., Ščevková, J., 2024. Comparative analysis of airborne fungal spore distribution in urban and rural environments of Slovakia. Environ. Sci. Pollut. Control Ser. 31, 63145–63160. https://doi.org/10.1007/s11356-024-35470-5.